ON THE USE OF EQUIVALENT LINEARIZATION FOR HIGH-CYCLE FATIGUE ANALYSIS OF GEOMETRICALLY NONLINEAR STRUCTURES

Stephen A. Rizzi
NASA Langley Research Center, Structural Acoustics Branch
Hampton, Virginia 23681-2199, USA. Email: s.a.rizzi@larc.nasa.gov

ABSTRACT

The use of stress predictions from equivalent linearization analyses in the computation of high-cycle fatigue life is examined. Stresses so obtained differ in behavior from the fully nonlinear analysis in both spectral shape and amplitude. Consequently, fatigue life predictions made using this data will be affected. Comparisons of fatigue life predictions based upon the stress response obtained from equivalent linear and numerical simulation analyses are made to determine the range over which the equivalent linear analysis is applicable.

INTRODUCTION

The design of advanced aerospace vehicle components capable of withstanding high vibroacoustic environments is hampered by a lack of accurate and computationally fast methods. Such methods are required in the design phase to quickly assess the impact of design changes on high-cycle fatigue life. In the past, linear analyses with a variety of scale factors have been utilized for this purpose. However, as vehicle performance and flight envelopes are expanded, the likelihood that the dynamic response may become geometrically nonlinear is increased, and the application of linear methods in these cases can lead to grossly conservative designs. The use of nonlinear dynamic response analyses is thus desirable not only from the standpoint of increased accuracy, but also to gain insight into the applicable mechanics.

Of the many methods in use to predict the geometrically nonlinear dynamic response of structures, equivalent linearization (EL) methods [1, 2] have seen broad application because of their ability to capture the response statistics over a wide range of response levels in a computationally efficient manner. Utilization of EL methods opens up the opportunity to incorporate nonlinear dynamic response and fatigue analyses in the design process. A recent finite element based implementation of EL [3] has been validated through an extensive nonlinear response range for beam [4] and plate [5] structures. The validation consisted of comparisons of displacements obtained from the EL analysis with those obtained from numerical integration in physical [4] and modal [5] coordinates. In both studies, root-mean-square (RMS) displacement responses compared favorably. The objective of this study is to determine the range over which fatigue life predictions based upon EL analysis results are valid.

High-cycle fatigue calculations are typically performed using a cumulative damage approach [6] and various cycle counting schemes. When stress/strain time histories are available, the rainflow cycle counting method [7] is often used. When time domain data are not available, then spectral fatigue methods may be used to approximate rainflow ranges from the stress/strain spectra [8]. The method employed to obtain stress/strain information in the present EL analysis provides stress/strain power spectral densities (PSD) of the equivalent linear system, not stress/strain time histories. Thus, the spectral fatigue method is dictated.

Spectral fatigue methods are well established for use with linear response data, but their use in the nonlinear response regime has not been fully verified. Therefore, before an assessment of the use of EL data can be made, the suitability of applying spectral fatigue methods in the nonlinear response regime must be determined using a consistent set of nonlinear data. The range of applicability will first be established by comparing fatigue life predictions made using a rainflow cycle counting analysis of nonlinear stress time histories, with predictions made using the spectral fatigue method with PSDs derived from these same nonlinear stress histories. Then, the range over which EL-based spectral fatigue life calculations are valid will be determined through comparison with life predictions made using the spectral fatigue method with nonlinear stress PSDs, over a range of nonlinear response.

RESPONSE ANALYSES

A clamped-clamped beam structure was selected for study because it exhibits the bending/membrane coupling behavior of interest when undergoing large deflection response. Further, its small system size makes numerical simulation tractable. The aluminum beam used had dimensions of 18-in. x 1-in. x 0.09in. (l x w x h) and the following material properties:

$$E = 10.6 \times 10^6\, psi, \qquad G = 4.0 \times 10^6\, psi, \qquad \rho = 2.588 \times 10^{-4}\, \frac{lb_f - s^2}{in^4}$$

The beam was subjected to a uniformly distributed loading with a bandwidth of 1500 Hz.

Equivalent Linearization Analysis. The EL analyses were performed using the program ELSTEP (Equivalent Linearization using a STiffness Evaluation Procedure) [3]. ELSTEP uses MSC.NASTRAN to determine the nonlinear modal stiffness coefficients by solving a series of linear and nonlinear static problems with prescribed displacements [5]. Two versions of the EL procedure are implemented. The traditional approach minimizes the difference between the nonlinear force and the product of the equivalent linear stiffness and displacement response. Results found using this approach will be designated by EL-FORCE. An alternative approach minimizes the error in strain energy. Results found using this approach will be designated as EL-STRAIN. Both approaches utilize the modal displacement response in the error minimization process. The outputs of ELSTEP are the RMS displacements and the equivalent linear modal stiffness.

Only the time history of quantities from the nonlinear system can be used to correctly obtain the nonlinear PSD, and this requires numerical simulation in either physical or modal coordinates. Such data are not available from the EL analysis. Thus, post-processing of EL analysis results, to generate information other than the RMS displacement and equivalent linear modal stiffness, is performed using *linear* analysis methods. Specifically, within a MSC.NASTRAN modal frequency response analysis (solution 111), the equivalent linear modal stiffness is substituted in place of the linear stiffness to obtain PSDs of the equivalent linear system. How useful such information is in a fatigue life calculation will be addressed in subsequent sections of this paper. What is known is that such a procedure generates a displacement PSD that bears little resemblance to the nonlinear displacement PSD, other than at low response levels, even though the RMS level is maintained [4, 5]. In particular, the equivalent linear displacement PSD does not exhibit peak broadening or the same peak shifting as found in the nonlinear system. The equivalent linear stress PSD differs from that of the nonlinear system in a similar fashion. There are however two additional factors affecting the quality of equivalent linear stress results. The first is that the *linear* post-processing operation employed is incapable of computing the membrane stress component, which exists only in the nonlinear system. Therefore, when the membrane stress is

comparable to, or exceeds the bending stress, the nonlinear stress PSD is noticeably affected while the equivalent linear stress PSD is not at all changed. Another important factor is that since the EL process is based upon the displacement response, the accuracy for computing derivatives of that response, i.e., stress or strain, is reduced. The end result is that equivalent linear stress spectra differ in both magnitude and shape from the nonlinear stress spectra and these differences will have an effect upon the fatigue life calculation.

The MSC.NASTRAN model used in the EL analysis was comprised of thirty-six ½-in. long CBEAM elements. A convergence check using ¼-in. elements showed the ½-in. elements to be adequate. The EL analysis used a four-mode solution comprised of the first four symmetric bending modes. Damping was chosen to be consistent with the mass-proportional damping of the numerical simulation analysis and sufficiently high so that a good comparison could be made at the peaks of the PSDs. A critical damping of 2.0% was chosen for the first mode, dictating values of 0.37%, 0.15%, and 0.081% for the next three symmetric modes.

Numerical Simulation Analysis. Numerical simulation analyses were performed using the finite element program NONSTAD [9] to generate nonlinear stress time histories from which fatigue life calculations were made. Numerical integration was performed in physical coordinates. The NONSTAD finite element model was also comprised of thirty-six ½-in. long beam elements. The mass proportional damping factor used was consistent with the damping specified in the EL analysis. The choice of NONSTAD over alternative analysis methods, e.g. MSC.NASTRAN nonlinear transient solution (solution 129), was made based on past successful application of NONSTAD for very long loading time histories [4]. Nearly identical nonlinear static stress analysis results from NASTRAN and NONSTAD (not shown) established a consistent comparison basis.

The loading time history was generated by summing equal amplitude sine waves with random phase within the specified bandwidth using a discrete inverse Fourier transform. This procedure was identical to that used in [4], so further details are omitted for brevity. The loading produced by this method has a Gaussian distribution. A sharp roll-off of the input spectrum practically eliminates excitation of the structure outside the frequency range of interest.

An explicit integration method with a Δt of $1\,\mu s$ was used for all load levels. Ten simulations of $2.1384s$ each were run at each load level and the first $0.5s$ of each were discarded to remove the initial transient response, by the method outlined in [4]. Each resulting response history had a $1.6384s$ duration. For each record, the response was stored at every $50\,\mu s$, giving a time record of 32,768 points. The longitudinal stress was separately output as membrane and bending components, with the bending component evaluated at the surface. Total stress was obtained by adding membrane and bending components in the time domain.

Response Results. Analyses were performed at load levels ranging from 7.2×10^{-3} to 0.9216 lb/in RMS to span a wide, yet practical, fatigue life range. Figure 1 shows the normalized RMS out-of-plane (v) deflection at the beam center as a function of load level. The numerical simulation results are shown with 90% confidence intervals of the RMS estimate. At the lowest load level of 7.2×10^{-3} lb/in RMS, the response is nearly linear as can be seen by the comparison with results from the linear analysis (NASTRAN solution 111). The degree of nonlinearity increases with increasing load level. EL force and strain error minimization analyses give comparable results to each other and agree well with numerical simulation results. At the highest load level, the nonlinear response calculations predict a RMS center deflection of roughly 1.8 times the thickness compared with the nearly 5.5 times the thickness from the linear analysis.

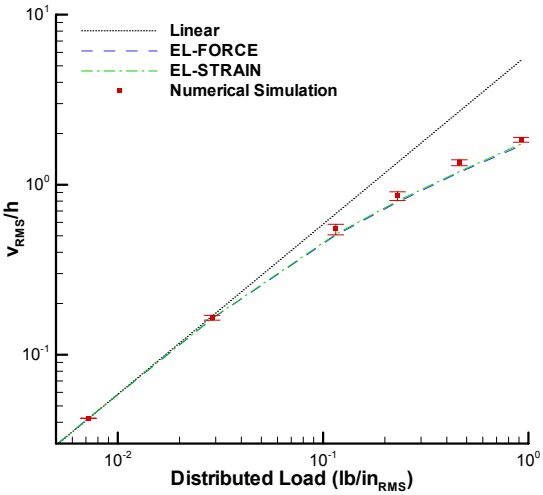

Figure 1: Normalized RMS center deflection as a function of load.

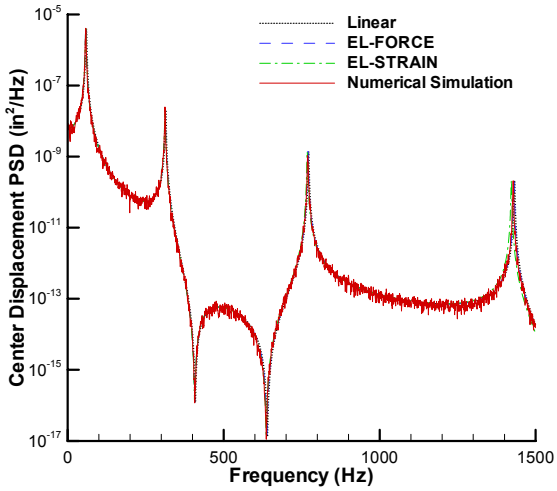

Figure 2: Center deflection response due to $7.2x10^{-3}$ lb/in distributed load.

The center displacement PSD is shown for the lowest load to highlight the manner in which the displacement response decreases with increasing frequency, see Figure 2. The EL displacement PSDs at higher response levels are shifted in frequency, but retain this characteristic [4, 5]. Since the equivalent linearization process utilizes the displacement response, the low frequency components are implicitly more heavily weighted than the high frequency components. A plot of the same information on a linear scale shows that the equivalent linear stiffness obtained through the EL process will be first bending mode dominated, see Figure 3. As a consequence, its use to predict quantities which are not low frequency dominated, e.g. stress, velocity and acceleration, gives less accurate results since any differences at the high frequencies are accentuated. This is evident in the RMS stress at the clamped end, as shown in Figure 4. Unlike the difference in RMS displacement, which is consistent for both EL approaches, the manner in which the EL RMS stresses differ from the nonlinear stress in not consistent between the two EL approaches. Such behavior precludes the use of a mechanics-based correction, so any scaling to match either of the EL RMS stresses with the RMS nonlinear stress will be ad hoc.

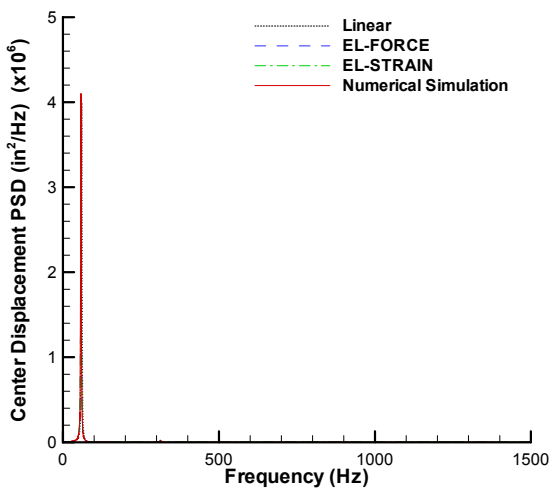

Figure 3: Center displacement response due to $7.2x10^{-3}$ lb/in load, on a linear scale.

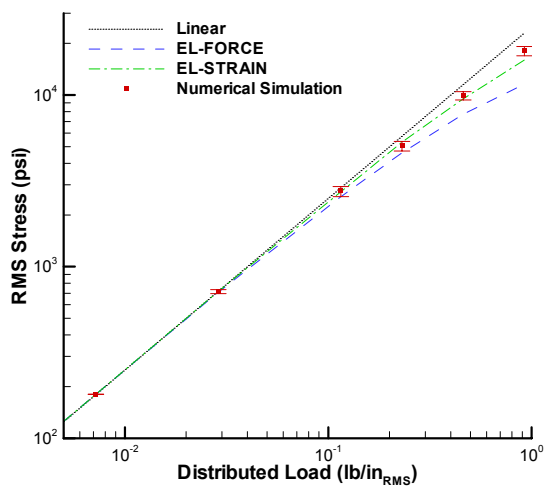

Figure 4: RMS stress at clamped end as a function of applied load.

Stress PSDs from the numerical simulation and EL analyses are shown in Figure 5 – Figure 8 for the clamped end at three levels spanning the load range. The lowest level, shown in Figure 5, is nearly linear and shows excellent agreement between the two EL analyses and the numerical simulation analysis, except at the anti-resonances. This is expected since numerical simulation in physical coordinates includes the contributions of the higher modes, which affect the anti-resonant behavior. The number of modes included in the EL analysis would need to be increased to capture this behavior. Since the fatigue life is determined by the peak behavior, no attempt was made to accurately capture this portion of the response.

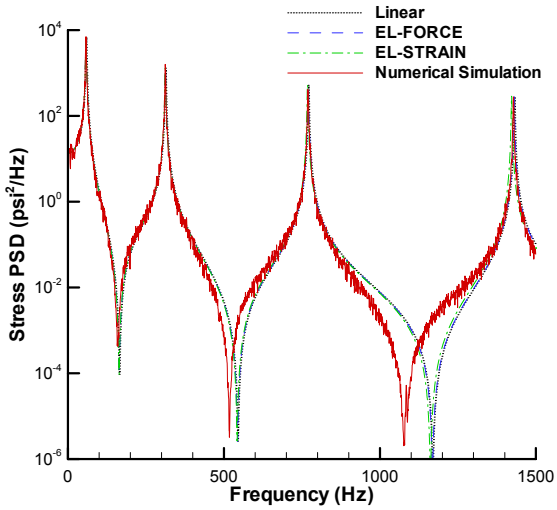

Figure 5: Stress PSDs at clamped end for $7.2x10^{-3}$ lb/in distributed load.

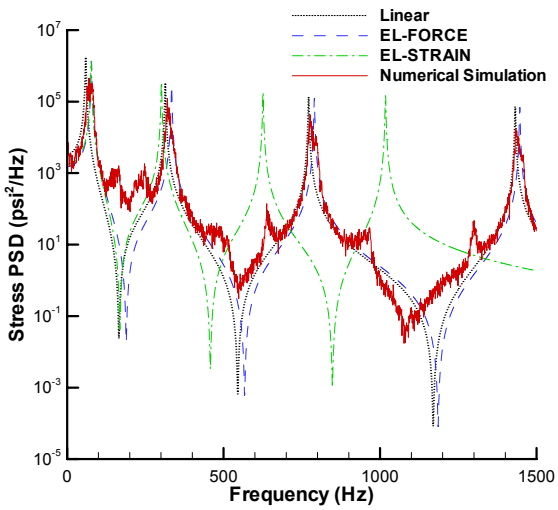

Figure 6: Stress PSDs at clamped end for 0.1152 lb/in distributed load.

At the moderately nonlinear level, the contribution of the membrane stress to the total stress is increased. This is evident in the nonlinear stress PSD which shows additional peaks from the membrane component at some frequencies, see Figure 6. The separate contributions of bending and membrane stress to the total stress (from the numerical simulation analysis) are shown for clarity in Figure 7. Some of the peaks in the membrane stress component are clearly recognizable as second harmonics of the dominant bending component. This is because for each fully reversed bending cycle, the membrane stress experiences two cycles between zero and the maximum positive value. Because the membrane stress is nearly constant along the length of the beam, the extent to which these additional peaks are introduced depends on the ratio of membrane to bending stress. At the clamped end, the bending stress is dominant over all load levels considered. Nearer to the locations of zero bending moment, the membrane component may dominate at the higher load levels. At the highest nonlinear response level, shown in Figure 8, peaks in the nonlinear stress PSD have become less discernible. What was the fourth mode has shifted in frequency outside of the analysis band. At both the moderately and highly nonlinear levels, peaks in the EL stress PSDs shift in frequency by differing amounts. Neither EL analysis shows the peak broadening behavior characteristic of the nonlinear response, nor are they able to compute the effect of the membrane component.

FATIGUE ANALYSIS OF NONLINEAR RANDOM RESPONSE

Under constant amplitude loading, the stress-life (*S-N*) curve relates the cycles to failure *N* to the applied stress range *S* via the relationship:

$$NS^m = K \tag{1}$$

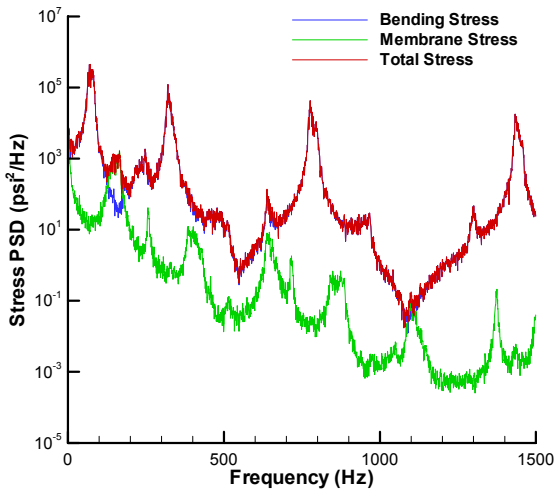

Figure 7: Contribution of bending and membrane stress to total (from Figure 6).

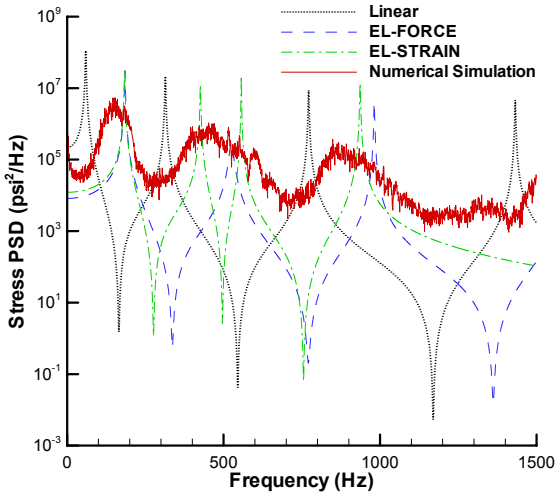

Figure 8: Stress PSDs at clamped end for 0.9216 lb/in distributed load.

where m and K are material specific properties. For variable amplitude loading, the Palmgren-Miner linear cumulative damage rule [6] is typically used and assumes that the damage, D, caused by stress cycles in one stress range can be calculated and added to damage caused by stress cycles in another stress range, or

$$D = \sum_i \frac{n_i}{N(S_i)} \tag{2}$$

where n_i is the number of cycles at stress range S_i, and $N(S_i)$ are the cycles to failure at stress range S_i. For random response, it is convenient to recast (2) in the alternative form

$$D = \frac{E[P]T}{K} \sum_i S_i^m P(S_i) \Delta S \tag{3}$$

where $P(S_i)$ is the stress range probability density function (PDF), ΔS is the PDF bin width, $E[P]$ is the number of peaks per second, and T is the lifetime. Failure is assumed to occur when the damage sums to 1, giving the fatigue life in seconds from (3) as

$$\text{Fatigue Life (s)} = \frac{K}{E[P] \sum_i S_i^m P(S_i) \Delta S} \tag{4}$$

Once the stress range PDF is found, it is a straightforward matter to calculate the fatigue life. In the time domain, a rainflow cycle counting analysis is typically used to obtain the stress range PDF. In the frequency domain, an approximation of the PDF is made. In the following, *S-N* properties for 7075-T6 aluminum were used with $m = 4.81$ and $K = 1.52 \times 10^{25}$.

Rainflow Analysis. At each loading level, ten total stress (bending and membrane) history records were joined together to form an overall record length of $T = 16.384s$ for the rainflow cycle counting analysis. The algorithm used [10] was provided as part of the Wave Analysis for Fatigue and Oceanography (WAFO) Matlab toolbox for analysis of random waves and loads [11]. The WAFO toolbox was used to compute the turning points for each stress time history, the rainflow cycles from the sequence of turning points, and the stress ranges from the

rainflow cycle count. The input stress time history data were not filtered. A histogram was computed from the stress ranges from which the stress range PDF was found by

$$P(S_i) = \frac{n_i}{S_t \Delta S} \tag{5}$$

where n_i are the histogram counts and S_t is the total number of rainflow cycles. The number of peaks per second, $E[P]$, was determined as

$$E[P] = \frac{S_t}{T} = \frac{S_t}{16.384s} \tag{6}$$

Spectral Fatigue Analysis. There are several approximations available to determine a stress range PDF for linear systems. Some are more appropriate to narrowband processes while others are more appropriate for broadband processes. A good comparison of several approximations may be found in [8]. For broadband processes, it is widely recognized that the Dirlik approximation [12] provides the best fit of the rainflow stress range PDF. Because of this, the Dirlik approximation was used as the basis for the present nonlinear analysis. It is possible that other formulations are more appropriate, but such an investigation is beyond the scope of this paper. Instead, the extent to which the Dirlik approximation is applicable to nonlinear systems will be investigated.

The Dirlik stress range PDF is given by

$$P(S_i) = \frac{\frac{D_1}{Q} e^{\frac{-z_i}{Q}} + \frac{D_2 z_i}{R^2} e^{\frac{-z_i^2}{2R^2}} + D_3 z_i e^{\frac{-z_i^2}{2}}}{2\sqrt{m_0}} \tag{7}$$

where

$$z_i = \frac{S_i}{2\sqrt{m_0}}, \qquad \gamma = \frac{E[0]}{E[P]}, \qquad E[0] = \sqrt{\frac{m_2}{m_0}}, \qquad E[P] = \sqrt{\frac{m_4}{m_2}}, \qquad x_m = \frac{m_1}{m_0}\sqrt{\frac{m_2}{m_4}}$$

$$D_1 = \frac{2\left(x_m - \gamma^2\right)}{1+\gamma^2}, \qquad D_2 = \frac{1-\gamma-D_1+D_1^2}{1-R}, \qquad D_3 = 1 - D_1 - D_2 \tag{8}$$

$$Q = \frac{1.25\left(\gamma - D_3 - D_2 R\right)}{D_1}, \qquad R = \frac{\gamma - x_m - D_1^2}{1-\gamma-D_1+D_1^2}$$

and m_0, m_1, m_2, and m_4 are the moments of the one-sided stress PSD $G(f)$ defined by

$$m_n = \sum_i f_i^n G(f_i)\Delta f \tag{9}$$

$G(f)$ is in units of stress^2/Hz (as shown in Figure 5, etc.) and f is the frequency in Hz. As in the fatigue life prediction using rainflow cycle counting, the total stress PSD (bending and membrane) was used to calculate the moments.

Fatigue Results. Stress range PDFs at the clamped end, ¼ span and ½ span locations are shown in Figure 9 for the lowest loading level. The higher stress ranges contribute most to the accumulated fatigue damage, and the Dirlik approximation compares very well with the rainflow stress range PDF in this regime. The fatigue life calculated at these three locations using the rainflow and Dirlik stress range PDFs are shown in Table 1 – Table 3. At the lowest

load level, the fatigue life computed with the Dirlik approximation is within 15% of the rainflow, with the greatest difference at the clamped end, the location of highest stress. The skewness and kurtosis were computed from the stress time histories, that is, they describe the shape of the stress PDF, not the stress range PDF. A near zero skewness and kurtosis close to 3 indicates a nearly linear response.

Table 1: Fatigue life at clamped end based on nonlinear response.

Load (lb/in)	Skewness	Kurtosis	Fatigue Life Rainflow	Fatigue Life Dirlik	Fatigue Life Ratio
0.0072	0.043	3.01	90.85 yr.	104.16 yr.	1.15
0.0288	0.117	2.97	41.71 days	54.24 days	1.30
0.1152	0.264	3.11	1.28 hr.	1.65 hr.	1.28
0.2304	0.358	3.69	2.50 min.	4.99 min.	2.00
0.4608	0.411	3.73	5.12 sec.	11.51 sec.	2.25
0.9216	0.440	4.19	0.16 sec.	0.33 sec.	2.06

In the moderately nonlinear response regime (0.1152 lb/in load), the stress range PDF obtained via the Dirlik approximation compares very well with the rainflow stress range PDF for the ¼ and ½ span locations, as shown in Figure 10. The corresponding fatigue life predictions using the Dirlik stress range PDF are within 7% of those computed using the rainflow stress range PDF. At the clamped end, larger differences are noted between the rainflow and Dirlik stress range PDFs. The Dirlik stress range PDF tends to underestimate the rainflow PDF in the high stress range portion of the distribution. This has the consequence of producing a somewhat non-conservative estimate of the fatigue life (see Table 1).

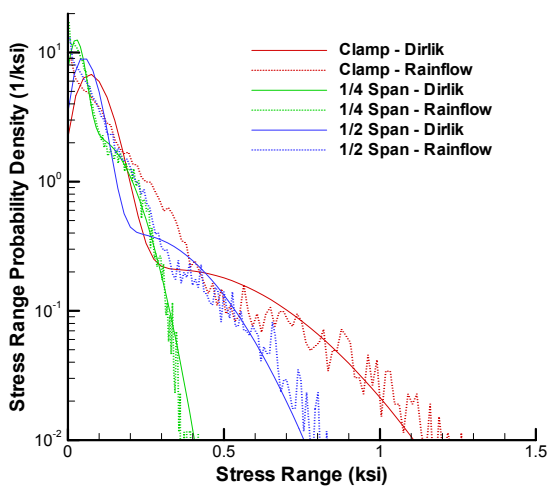

Figure 9: Stress range PDFs of nonlinear response prediction at $7.2x10^{-3}$ lb/in load.

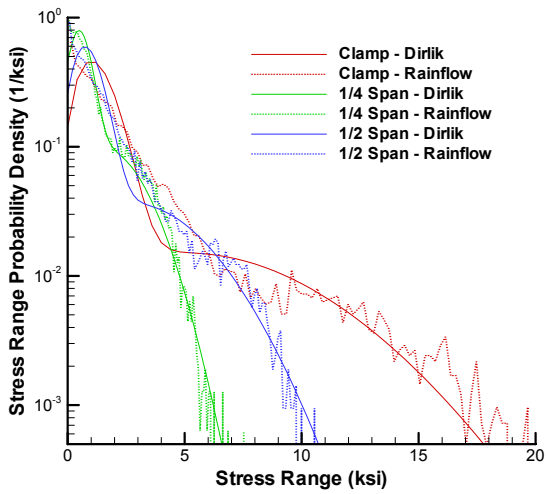

Figure 10: Stress range PDFs of nonlinear response prediction at 0.1152 lb/in load.

Finally, in the highly nonlinear response regime (0.9216 lb/in load), the Dirlik distributions in the high stress ranges are slightly higher than the rainflow distributions for the ¼ and ½-span locations, as shown in Figure 11. This has the effect of giving a conservative fatigue life estimate. The Dirlik distribution for the clamped end, however, is lower than the rainflow distribution in the high stress range, resulting in a non-conservative fatigue life estimate.

At all three locations, the skewness of the total nonlinear stress PDF increases from near zero to a positive value due to the increasing contribution of the membrane stress component to the total stress. The membrane stress component takes on a Rayleigh distribution since it

oscillates between zero at the neutral position and a positive value for either upward or downward bending (see Figure 12, for example) while the bending stress remains more or less Gaussian. An increasing kurtosis value indicates a sharpening of the stress PDF. This is most pronounced at the clamped end, and may be related to the largest differences noted in the fatigue life prediction.

Table 2: Fatigue life at ¼-span based on nonlinear response.

Load (lb/in)	Skewness	Kurtosis	Fatigue Life Rainflow	Fatigue Life Dirlik	Fatigue Life Ratio
0.0072	0.009	2.84	12536 yr.	11475 yr.	0.92
0.0288	0.047	2.98	14.89 yr.	16.71 yr.	1.12
0.1152	0.192	3.13	7.63 days	8.19 days	1.07
0.2304	0.301	3.22	7.15 hr.	7.20 hr.	1.01
0.4608	0.378	3.15	20.73 min.	18.43 min.	0.89
0.9216	0.535	3.52	44.64 sec.	37.18 sec.	0.83

Table 3: Fatigue life at ½-span based on nonlinear response.

Load (lb/in)	Skewness	Kurtosis	Fatigue Life Rainflow	Fatigue Life Dirlik	Fatigue Life Ratio
0.0072	0.033	2.99	683.68 yr.	760.52 yr.	1.11
0.0288	0.145	2.92	0.95 yr.	1.13 yr.	1.19
0.1152	0.348	2.82	22.18 hr.	21.03 hr.	0.95
0.2304	0.368	2.97	1.12 hr.	1.19 hr.	1.07
0.4608	0.336	2.81	4.73 min.	4.10 min.	0.88
0.9216	0.445	3.24	14.42 sec.	11.64 sec.	0.81

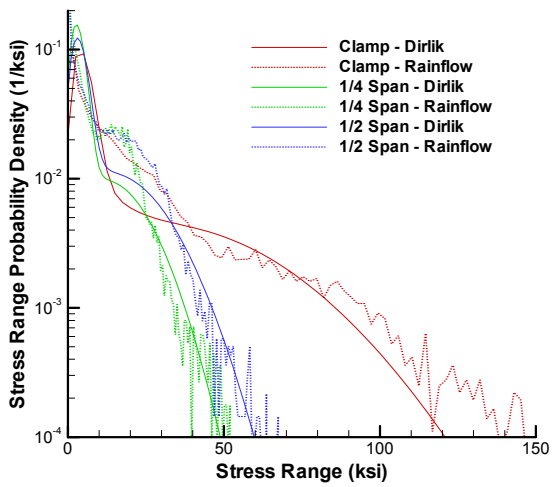

Figure 11: Stress range PDFs of nonlinear response prediction at 0.9216 lb/in load.

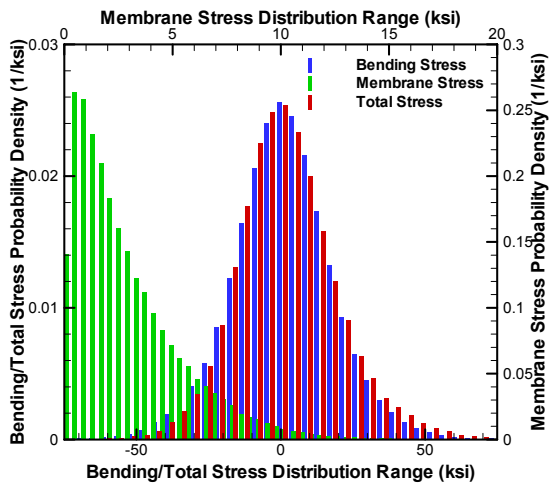

Figure 12: Nonlinear stress PDF at clamped end for 0.9216 lb/in load.

The larger differences noted in the fatigue life predictions at the higher response levels indicate a need for a correction to the Dirlik formula to account for nonlinearity. Development of a correction is beyond the scope of this effort, but is being undertaken elsewhere [13]. However, in order to put these differences into perspective, it is helpful to look at the confidence interval in the nonlinear stress prediction. At the highest load level, the 90% confidence interval of the stress at the clamped end is 16.94 ksi RMS – 19.19 ksi RMS (see Figure 4). The corresponding fatigue life prediction using the rainflow derived stress

range PDFs varies from 0.226*s* to 0.124*s*, almost a factor of 2. Therefore, while differences exist between fatigue life predictions made using the Dirlik approximation and rainflow counting methods, these differences are on the order of those due to uncertainty in the simulated stress history. Lastly, from a practical standpoint, the difference in fatigue life in absolute terms is much smaller at the higher response levels with higher error, than the difference at lower response levels with smaller error. Having established some confidence in the use of the Dirlik approximation in the nonlinear regime, fatigue life predictions using the Dirlik approximation based on equivalent linear response data is next undertaken.

FATIGUE ANALYSIS OF EQUIVALENT LINEAR RESPONSE

The stress range PDFs based on EL-FORCE stress PSDs are shown in Figure 13 – Figure 15 for the nearly linear, moderately nonlinear, and highly nonlinear cases. For comparison, the nonlinear stress range PDFs using the Dirlik approximation are also shown. Figure 13 shows the stress range PDF for the nearly linear level. Close agreement of the stress range PDF results in comparable fatigue life, as indicated in Table 4. The EL-FORCE and nonlinear stress range PDFs are shown to differ at the moderately nonlinear level, as shown in Figure 14. For each location, the EL-FORCE stress range PDF is higher in the mid-stress range and lower in the more important high stress range, relative to the nonlinear stress range PDF. This produces a non-conservative fatigue life prediction, as shown in Table 4. The highly nonlinear level, shown in Figure 15, indicates the difference is more pronounced but with similar character.

Table 4: Dirlik fatigue life prediction based on EL-FORCE response.

Load (lb/in)	Dirlik Fatigue Life Prediction			Fatigue Life Ratio (relative to Dirlik nonlinear response)		
	Clamp	¼ Span	½ Span	Clamp	¼ Span	½ Span
0.0072	108.84 yr.	12733 yr.	795.08 yr.	1.04	1.11	1.05
0.0288	53.00 days	16.88 yr.	1.12 yr.	0.98	1.01	0.98
0.1152	2.18 hr.	10.93 days	21.40 hr.	1.32	1.33	1.02
0.2304	6.32 min.	14.65 hr.	1.25 hr.	1.27	2.03	1.04
0.4608	29.01 sec.	225.39 min.	7.61 min.	2.52	12.2	1.86
0.9216	3.62 sec.	4.96 hr.	101.57 sec.	10.82	480	8.72

The stress range PDFs based on EL-STRAIN stress PSDs are shown in Figure 16 and Figure 17 for the moderately nonlinear and highly nonlinear cases, respectively. The nearly linear case does not differ significantly from Figure 13. At the moderately nonlinear level, the EL-STRAIN stress range PDF exceeds the nonlinear stress range PDF over the majority of the stress range and produces a conservative estimate of the fatigue life at each location. For the most part, this is also the case at the highest level, with the EL-STRAIN stress range PDF exceeding the nonlinear stress range PDF only at the highest stress range at the clamped end. This results in a non-conservative fatigue life prediction at that point. Dirlik fatigue life predictions based on the EL-STRAIN stress PSDs are summarized in Table 5.

The most significant quantity is the fatigue life at the clamp, as it dictates the life of the structure. For this problem, it is seen that the fatigue life prediction based on the EL-FORCE response does reasonably well through all but the highest nonlinear response, with a bias toward the non-conservative side through the range of response levels. Fatigue life predictions based on the EL-STRAIN response also do reasonably well through the response range, but with a bias predominantly toward the conservative side.

Table 5: Dirlik fatigue life prediction based on EL-STRAIN response.

Load (lb/in)	Dirlik Fatigue Life Prediction			Fatigue Life Ratio (relative to Dirlik nonlinear response)		
	Clamp	¼ Span	½ Span	Clamp	¼ Span	½ Span
0.0072	108.37 yr.	12606 yr.	791.20 yr.	1.04	1.10	1.04
0.0288	49.93 days	14.76 yr.	1.03 yr.	0.92	0.88	0.91
0.1152	1.52 hr.	5.09 days	13.94 hr.	0.93	0.62	0.66
0.2304	2.77 min.	3.81 hr.	0.40 hr.	0.55	0.53	0.33
0.4608	8.22 sec.	10.24 min.	1.12 min.	0.71	0.56	0.27
0.9216	0.52 sec.	33.11 sec.	3.78 sec.	1.57	0.89	0.32

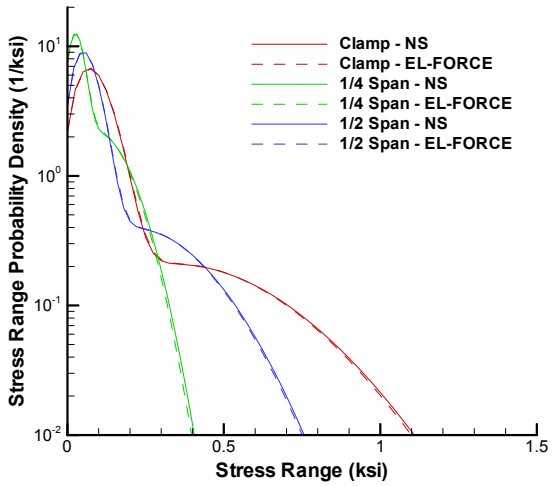

Figure 13: Dirlik stress range PDFs of EL-FORCE response at $7.2x10^{-3}$ lb/in load.

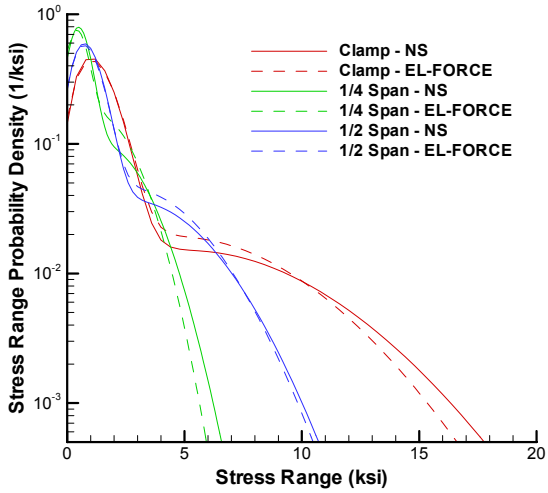

Figure 14: Dirlik stress range PDFs of EL-FORCE response at 0.1152 lb/in load.

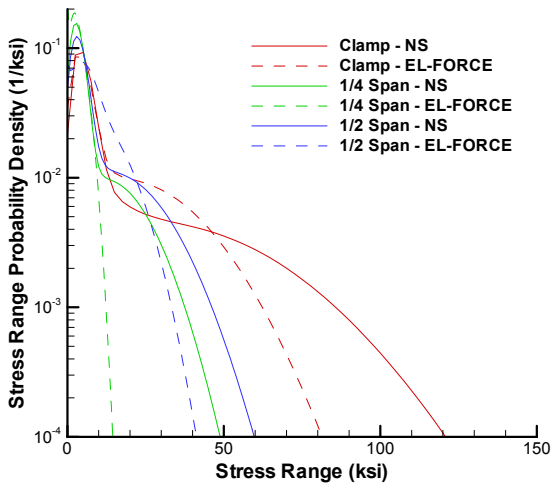

Figure 15: Dirlik stress range PDFs of EL-FORCE response at 0.9216 lb/in load.

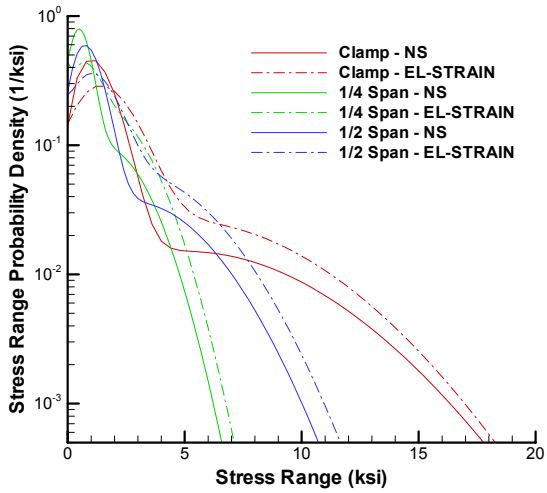

Figure 16: Dirlik stress range PDFs of EL-STRAIN response at 0.1152 lb/in load.

Effect of Mean Stress. A thorough treatment of mean stress effects is beyond the scope of this work. It is however worthwhile to consider how this analysis might be performed within the context of an equivalent linearization analysis. In the absence of steady-state thermal or mechanical loadings, the mean stress response is due to the membrane stress, as generated by bending-membrane coupling. For situations in which the total stress is bending stress dominated, the cyclic behavior of the membrane component likely plays an insignificant role in fatigue damage accumulation. Therefore, the net effect of the membrane stress is to shift

the stress ratio R ($\sigma_{\min} / \sigma_{\max}$) from fully reversed bending (R = -1) toward R = 0, requiring use of an alternative *S-N* curve. For a numerical simulation analysis, R may be determined in a straightforward manner. This is not the case for the EL analysis, as the membrane stress is unknown. An approximate means of determining R would be to run a series of nonlinear static analyses over an extended load range. Then at any particular location on the structure, the membrane to bending stress ratio may be obtained as a function of displacement, as shown in Figure 18. By equating the static displacement with the equivalent linear RMS displacement at the desired load level, an estimate of the equivalent linear RMS stress ratio may be obtained, through which the value of R may be found. The validity of this approach hinges upon how well the dynamic RMS stress ratio resembles the nonlinear static stress ratio, and this remains to be determined.

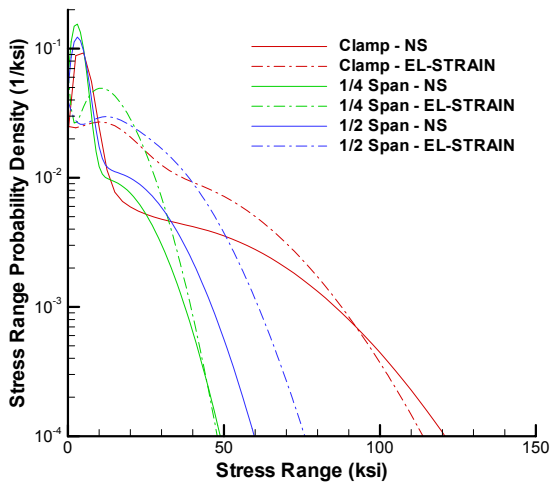

Figure 17: Dirlik stress range PDFs of EL-STRAIN response at 0.9216 lb/in load.

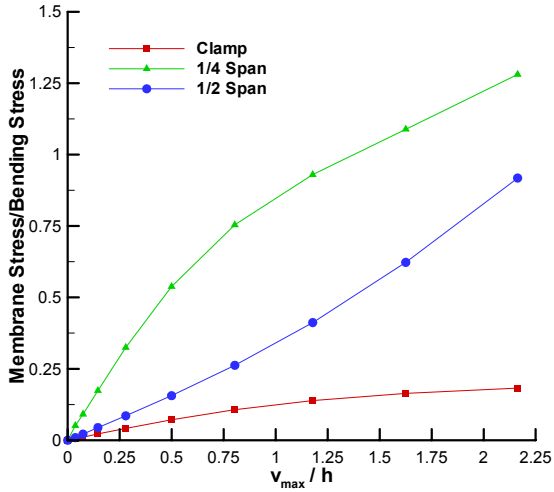

Figure 18: Nonlinear static stress ratio for estimating stress ratio R.

CONCLUDING REMARKS

The use of equivalent linear stress response in high-cycle fatigue prediction has been examined. Because the equivalent linearization process is performed using modal displacements, the low frequency contribution is more heavily weighted. As a consequence, using the so-obtained equivalent linear stiffness in the computation of quantities with more significant high frequency content such as stress results in reduced accuracy. Though outside the scope of this work, this suggests an alternative approach to the equivalent linearization process in which the appropriate time derivatives of the displacement would be used to affect the frequency weighting, i.e. displacement for low frequency weighting, velocity of a more even weighting, and acceleration for high frequency weighting. In the computation of stress, it is suggested that velocity be used.

An assessment of the spectral fatigue method in the nonlinear response regime was made so that subsequent fatigue life calculations made using the EL stress response could be compared on the same basis as those made using the nonlinear stress response. The Dirlik approximation for the stress range PDF produced fatigue life estimates within roughly a factor of two compared with prediction from the rainflow cycle counting method at the highest nonlinear levels. While this degree of accuracy was adequate for demonstrating its usefulness in subsequent comparisons, an improvement to the model for use in the nonlinear response regime would be beneficial.

Equivalent linear stress PSDs differ in overall magnitude and shape from the nonlinear stress response. Therefore, it should come as no surprise that fatigue life predictions based upon

them were found to differ from life predictions made using the nonlinear stress response. Except at the highest nonlinear response levels, these differences are on the order of differences due to other factors including confidence in the nonlinear stress predictions and differences between rainflow and spectral fatigue prediction methods. From these results, it is apparent that the linear cumulative damage law is insensitive to differences in the stress range distribution. Contrary to the underlying mechanics, the details of the distribution are important only to the extent that the summation in (4) yields similar values. The differences noted between fatigue life predictions made using equivalent linear stress PSDs and predictions made from nonlinear analysis should not preclude the use of EL based life predictions in the design environment. For fast, comparative analyses, the fidelity of such predictions may be more than adequate. When used in conjunction with a full nonlinear analysis for final assessments, significant time savings may be realized.

ACKNOWLEDGEMENTS

The author wishes to thank Professor James F. Doyle of Purdue University for providing the finite element code NONSTAD used for the numerical simulation analysis, for his advice on its use, and for other helpful suggestions.

REFERENCES

[1] Caughy, T.K., "Equivalent linearization techniques," *Journal of the Acoustical Society of America*, Vol. 35, pp. 1706-1711, 1963.

[2] Roberts, J.B. and Spanos, P.D., *Random vibration and statistical linearization*. New York, NY, John Wiley & Sons, 1990.

[3] Rizzi, S.A. and Muravyov, A.A., "Improved equivalent linearization implementations using nonlinear stiffness evaluation," NASA TM-2001-210838, March 2001.

[4] Rizzi, S.A. and Muravyov, A.A., "Comparison of nonlinear random response using equivalent linearization and numerical simulation," *Structural Dynamics: Recent Advances, Proceedings of the 7th International Conference*, Vol. 2, pp. 833-846, Southampton, England, 2000.

[5] Rizzi, S.A. and Muravyov, A.A., "Equivalent linearization analysis of geometrically nonlinear random vibrations using commercial finite element codes," NASA TP-2002-211761, July 2002.

[6] Miner, M.A., "Cumulative damage in fatigue," *Trans. ASME, Journal of Applied Mechanics*, Vol. 67, pp. A159-A164, 1945.

[7] Matsuishi, M. and Endo, T., "Fatigue of metals subjected to varying stress," *Japan Society of Mechanical Engineers*, Fukuoka, Japan, 1968.

[8] Bouyssy, V., Naboishikov, S.M., and Rackwitz, R., "Comparison of analytical counting methods for Gaussian processes," *Structural Safety*, Vol. 12, pp. 35-57, 1993.

[9] Doyle, J.F., *Nonlinear analysis of thin-walled structures*. New York, Springer, 2001.

[10] Rychlik, I., "A new definition of the rainflow cycle counting method," *International Journal of Fatigue*, Vol. 9, No. 2, pp. 119-121, 1987.

[11] "WAFO - A Matlab toolbox for analysis of random waves and loads," Version 2.0.02, The WAFO Group, Lund Institute of Technology, Lund University, 2000.

[12] Dirlik, T., "Application of computers in fatigue analysis," *Ph.D. Thesis*, Warwick University, 1985.

[13] Sweitzer, K.A., Veltri, M., Kerr, S.C., and Bishop, N.W.M., "A preliminary application of the PDF transfer function to fatigue calculations for nonlinear systems," *Structural Dynamics: Recent Advances, Proceedings of the 8th International Conference*, Southampton, England, 2003.